Journal of Toxicology and Environmental Health, Part A: Current Issues

Publication details, including instructions for authors and subscription information:
http://www.tandfonline.com/loi/uteh20

Pulmonary and Cardiovascular Responses of Rats to Inhalation of Silver Nanoparticles

Jenny R. Roberts [a], Walter McKinney [a], Hong Kan [a], Kristine Krajnak [a], David G. Frazer [a], Treye A. Thomas [b], Stacey Waugh [a], Allison Kenyon [a], Robert I. MacCuspie [c], Vincent A. Hackley [c] & Vincent Castranova [a]

[a] National Institute for Occupational Safety and Health , Morgantown , West Virginia , USA
[b] U.S. Consumer Product Safety Commission , Bethesda , Maryland , USA
[c] National Institute of Standards and Technology , Gaithersburg , Maryland , USA
Published online: 13 Aug 2013.

To cite this article: Jenny R. Roberts , Walter McKinney , Hong Kan , Kristine Krajnak , David G. Frazer , Treye A. Thomas , Stacey Waugh , Allison Kenyon , Robert I. MacCuspie , Vincent A. Hackley & Vincent Castranova (2013) Pulmonary and Cardiovascular Responses of Rats to Inhalation of Silver Nanoparticles, Journal of Toxicology and Environmental Health, Part A: Current Issues, 76:11, 651-668, DOI: 10.1080/15287394.2013.792024

To link to this article: http://dx.doi.org/10.1080/15287394.2013.792024

Journal of Toxicology and Environmental Health, Part A, 76:651–668, 2013
ISSN: 1528-7394 print / 1087-2620 online
DOI: 10.1080/15287394.2013.792024

Taylor & Francis
Taylor & Francis Group

PULMONARY AND CARDIOVASCULAR RESPONSES OF RATS TO INHALATION OF SILVER NANOPARTICLES

Jenny R. Roberts[1], Walter McKinney[1], Hong Kan[1], Kristine Krajnak[1], David G. Frazer[1], Treye A. Thomas[2], Stacey Waugh[1], Allison Kenyon[1], Robert I. MacCuspie[3], Vincent A. Hackley[3], Vincent Castranova[1]

[1]National Institute for Occupational Safety and Health, Morgantown, West Virginia, USA
[2]U.S. Consumer Product Safety Commission, Bethesda, Maryland, USA
[3]National Institute of Standards and Technology, Gaithersburg, Maryland, USA

Exposure to wet aerosols generated during use of spray products containing silver (Ag) has not been evaluated. The goal was to assess the potential for cardiopulmonary toxicity following an acute inhalation of wet silver colloid. Rats were exposed by inhalation to a low concentration (100 μg/m^3) using an undiluted commercial antimicrobial product (20 mg/L total silver; approximately 33 nm mean aerodynamic diameter [MAD]) or to a higher concentration (1000 μg/m^3) using a suspension (200 mg/L total silver; approximately 39 nm MAD) synthesized to possess a similar size distribution of Ag nanoparticles for 5 h. Estimated lung burdens from deposition models were 0, 1.4, or 14 μg Ag/rat after exposure to control aerosol, low, and high doses, respectively. At 1 and 7 d postexposure, the following parameters were monitored: pulmonary inflammation, lung cell toxicity, alveolar air/blood barrier damage, alveolar macrophage activity, blood cell differentials, responsiveness of tail artery to vasoconstrictor or vasodilatory agents, and heart rate and blood pressure in response to isoproterenol or norepinephrine, respectively. Changes in pulmonary or cardiovascular parameters were absent or nonsignificant at 1 or 7 d postexposure with the exceptions of increased blood monocytes 1 d after high-dose Ag exposure and decreased dilation of tail artery after stimulation, as well as elevated heart rate in response to isoproterenol 1 d after low-dose Ag exposure, possibly due to bioavailable ionic Ag in the commercial product. In summary, short-term inhalation of nano-Ag did not produce apparent marked acute toxicity in this animal model.

Nanoparticulate ("nano") silver (Ag) and nano anatase titanium dioxide (TiO_2) exhibit antimicrobial properties. These antimicrobial properties are being exploited by the incorporation of these nanoparticles into numerous commercial products, including disinfectants, filters, odor-resistant clothing, bandages, and medical devices (Wijnoven et al., 2009). The antimicrobial properties of nano anatase TiO_2 have been associated with the generation of reactive oxygen species (ROS) in the presence of ultraviolet light (Xue et al., 2010), while the antimicrobial action of nano Ag particles is due to the dissolution into ionic Ag and resultant oxidant injury to the microbes (Kittler et al., 2010). The active properties of these nanomaterials render them particularly useful as spray products, such as sunscreens, deodorants, surface disinfectants, and topical medical sprays. Potential exposure to the nanomaterials

Received 18 December 2012; accepted 30 March 2013.
This project was supported in part by an Interagency Agreement (CPSC-I-11-005) from the U.S. Consumer Product Safety Commission to the National Institute for Occupational Safety and Health. The findings and conclusions in this article are those of the authors and do not necessarily represent the view of the National Institute for Occupational Safety and Health or the U.S. Consumer Product Safety Commission.
Address correspondence to Jenny R. Roberts, PhD, Health Effects Laboratory Division (HELD), National Institute for Occupational Safety and Health (NIOSH), Centers for Disease Control and Prevention (CDC), 1095 Willowdale Rd. (M/S 2015), Morgantown, WV 26505, USA. E-mail: jur6@cdc.gov

contained in these products and the effects of the exposures are of concern in both worker and consumer product end use.

There are few data available in regard to emissions of Ag from spray products. A study by Quadros and Marr (2011) examined size and amount of Ag contained in three different Ag spray products that varied in application purpose (anti-odor spray, surface disinfectant, and throat spray), concentration, and particle size distribution. The form in which Ag was present in these sprays (elemental, ionic, in compound with other contaminants) was not well described by the manufacturers with the exception of the throat spray, which was described as colloidal Ag. Quadros and Marr (2011) calculated a range of 0.24–55.6 ng per spray action of the various cans and estimated the lung burdens that might result from a single use of the products (60–70 ng). However, to date, there are no apparent measures available in the breathing zone of workers during use of Ag spray products, which may likely result in exposure to greater amounts of the products.

Recently, Chen et al. (2010) characterized the generation of TiO_2 particles during the use of an antimicrobial spray product containing nano anatase. Results indicated that particulate levels in the breathing zone of an individual applying the spray to a vertical surface might reach 3.4 mg/m^3, with most of these TiO_2 particles being less than 110 nm in diameter. Results of a rat study with inhalation of this TiO_2 spray demonstrated a dose-dependent increase in breathing rate, pulmonary inflammation, and lung cell injury 24 h after exposure (3.79 mg/m^3, 4 h/d, 4 d) (McKinney et al., 2012). To evaluate the potential effects of aerosol exposure to Ag spray, a similar inhalation study was performed. The objectives of the current study were to (1) design and construct an aerosol generation system for an antimicrobial nano Ag consumer spray product; (2) characterize the wet aerosol generated; and (3) determine pulmonary and cardiovascular responses to an acute inhalation of Ag nanoparticles using a rat model.

Numerous commercial spray products containing Ag claim to be colloidal in nature (particles in suspension), although the degree to which these claims are true colloids is questionable, and these products may contain Ag in its ionic form or bound to other compounds. An antifungal spray (MesoSilver) was selected for this study as it was reported by the manufacturer to be a true colloid (predominantly Ag particles with low free ion concentration), and the particle size and concentration were also provided by the manufacturer. In addition, to attain a higher dose exposure, a second Ag colloid was provided by the National Institute for Standards and Technology (NIST). An aerosol delivery system was designed to maintain a constant level of exposure to a "wet" aerosol. Rats were exposed for 5 h to a low dose (100 μg/m^3 using the commercial colloid sprayer, high (1000 μg/m^3) dose of Ag spray using the colloid provided by NIST, or sterile deionized water as a control spray. The low dose was selected to be equivalent to the threshold limit value time-weighted average (TLV-TWA) set by the American Conference of Governmental Industrial Hygienists (ACGIH) for particulate Ag. It is well understood from epidemiological studies that pulmonary particulate matter (PM) exposure has been associated with adverse cardiovascular effects (Pope et al., 1995, 2002; Samet et al., 2000; Liao et al., 2011; Beckerman et al., 2012; Hsieh et al., 2010). More recently, respiratory exposure to various nanoparticles in animal models was also found to produce cardiovascular responses (Mann et al., 2012; Simeonova and Erdely, 2009), which are at times present in the absence of pulmonary measures toxicity (Nurkiewicz et al., 2008). Therefore both pulmonary and cardiovascular indices of toxicity were examined at 1 and 7 d after exposure to Ag sprays.

MATERIALS AND METHODS

Ag Nanoparticles

Two sources of Ag nanoparticles were used in this study. The first was an advertised antimicrobial product purchased from the company website (MesoSilver, Purest Colloids,

Inc., Westampton, NJ).[1] Company data indicated that the product was a deionized water solution containing 20 mg/L total Ag (75% colloidal silver and 25% silver ions; primary Ag nanoparticle size was described as 0.65 nm). The second Ag nanoparticle sample was synthesized at National Institute of Standards and Technology (NIST) (approximately 100% colloidal; approximately 1000 mg/L stock concentration Ag in deionized water), synthesized as described by MacCuspie et al. (2011). Particle size and concentration were characterized at NIST using dynamic light scattering (DLS) and ultraviolet–visible (UV-vis) absorbance, using a Zetasizer Nano (Malvern Instruments, Westborough, MA) and a Lambda 750 (Perkin Elmer, Waltham, MA), respectively. Samples were measured in a semimicro disposable cuvette transferred between instruments immediately after completion. DLS data from 5 consecutive measurements are reported as the mean ± 1 standard deviation of the *Z*-average diameter, reflecting the repeatability of the measurements and not the width of the size distribution.

The commercial product had a trimodal size distribution with peaks at 3, 20, and 150 nm, indicating a polydisperse distribution. The average diameter of this preparation was 55.7 ± 1.2 nm. UV-vis spectra indicated that 4.23 mg/L of the solution was in particulate form, relative to the 20 mg/L total Ag concentration reported by the manufacturer. It is noteworthy that sizes less than 1 nm as reported by the manufacturer may not be detected by DLS, and that the lower limit of detection for this model of UV-vis spectraphotometer is 0.17 nm. Therefore, a greater portion of the sample was either below the limit of detection or a greater percentage of the solution was ionic in nature. DLS data of the NIST colloid showed a bimodal size distribution with peaks at 3 and 40 nm. The average diameter was 15.2 ± 0.1 nm. UV-vis spectra confirmed a particulate concentration of 1030 mg/L. Prior to aerosolization, the NIST sample was diluted further to a concentration of 200 mg/L in sterile deionized water so that one order of magnitude difference in concentration would exist between the two samples, representing a high and low dose of Ag spray aerosol. In addition, scanning electron microscope (SEM) images of the aerosols for both the high- and low-dose samples were collected through the inhalation system. The SEM measures verified the DLS data showing that the fraction of the low-dose sample with diameter of less than 1 nm was minor. For the high-dose sample, the SEM data showed particle sizes to be slightly greater than the mean determined by DLS. Data are discussed in greater detail below.

[1]Certain trade names and company products are mentioned in order to adequately specify the experimental procedures and equipment used. In no case does such identification imply recommendation or endorsement by the National Institute of Standards and Technology (NIST), nor does it imply that the products are necessarily the best available for the purpose.

Exposure System

An inhalation exposure system was designed and assembled to generate wet aerosols that were representative of those produced while using spray-on Ag products. The exposure system requirements were to: (1) deliver a wet aerosol of small H_2O droplets, typically less than 150 nm diameter, comprised of nanosized Ag particles and Ag ions to the animal's breathing space; (2) maintain automatically constant exposure levels (number of particles per milliliter) within the exposure chamber while minimizing fluctuations; (3) control automatically chamber pressure, air flows, and total exposure time; and (4) monitor and record the temperature and humidity within the exposure chamber.

A block diagram of the nano-Ag spray aerosol inhalation exposure system is shown in Figure 1. Air from the NIOSH facility's water seal compressor was conditioned by passing it through a dryer, a charcoal filter, and then a HEPA filter. This clean air was then regulated down to a pressure of 0.24 MPa (35 pounds per square inch [PSI]) to provide air to two calibrated rotameter flow controllers (10 L/min each, Dwyer Instruments, Michigan City, IN) and to two model 3076 aerosol generators (3 L/min each) (TSI, Inc., Shoreview, MN). The

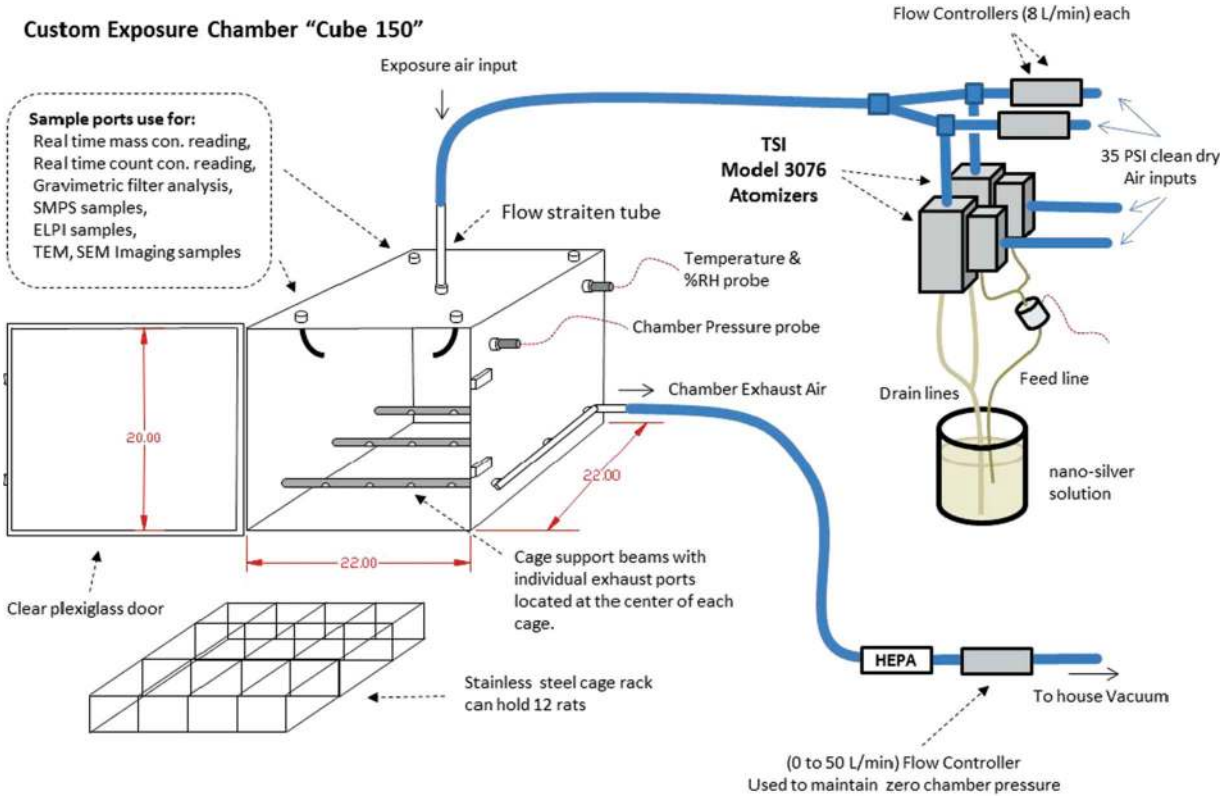

FIGURE 1. Diagram of the computer controlled nano-silver spray aerosol exposure system. Dimensions of the chamber are given in inches (color figure available online).

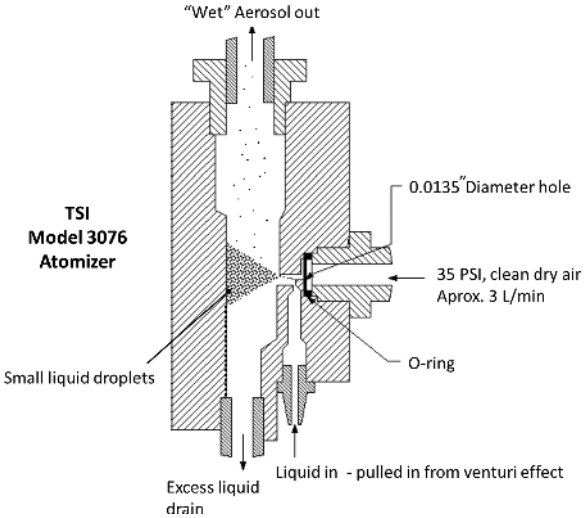

FIGURE 2. Diagram of the TSI 3076 aerosol generator.

TSI 3076 aerosol generators, shown in Figure 2, were collision-type atomizers that generated wet aerosols from a solution in the form of small droplets (less than 200 nm in diameter). During an exposure, one of the two Ag suspensions was pulled passively into the generators via vacuum pressure created by high-velocity airflows through a 0.343-mm (0.0135-inch) diameter hole (Figure 2). A computer-controlled valve (Cole Parmer Instruments) was used to distribute the supply of solution to the generators as needed. Excess fluid within the generators was returned to the solution through drain lines. Output air from the two aerosol generators was mixed with the clean dry air from the two flow controllers, resulting in a total flow of 26 L/min being delivered to the exposure chamber. This flow (26 L/min) was used to provide adequate exposure chamber air changes per hour to maintain CO_2, ammonia, temperature, and relative humidity within acceptable levels. A custom-built 150-L stainless-steel exposure chamber (Cube 150), capable of accommodating 12 rats within individual cage partitions, was used. A condensation particle counter (CPC model 3775,

TSI, Inc., Shoreview, MN) was used to monitor continuously the particle-count concentration within the exposure chamber, and an instrument based on light scattering properties of aerosols (DataRAM 4, Thermo Scientific, Franklin, MA) was used to monitor continuously the mass concentration of Ag particles inside the exposure chamber. Dry Ag aerosol concentrations were determined gravimetrically with 37-nm cassettes containing Teflon filters and used to calibrate and verify the DataRAM readings after each exposure run. After the aerosol exited the exposure chamber, it was passed through a HEPA filter, and the air was exhausted through a mass flow controller to a vacuum system. The pressure inside the exposure chamber was measured continuously with a pressure transducer (Serta, model 264, Serta Sensing Solution, Boxborough, MA). The exposure system's control software was designed to make adjustments automatically to the exhausted flow controller to keep the exposure chamber at a negative pressure of −12 Pa (−0.05 inches H_2O). This slight negative pressure was maintained to minimize air leaks and to aid in preventing the aerosol from escaping the exposure chamber into the room. The temperature and humidity of the air inside the exposure chamber were measured continuously with a temperature/humidity sensor (Vaisala, model 234, Boulder, CO).

Inhalation Exposures

Table 1 describes the three exposure conditions used in this study. The 20-mg/L concentration representing the total Ag in the commercial product was the value used for the low-dose sample for aerosol calculations, although a portion of this was likely ionic in nature, as discussed earlier. For the high-dose sample synthesized at NIST the stock solution with 1030 mg/L concentration was diluted in sterile deionized water to a weight of 200 mg/L for aerosolization. Number of particles in the exposure airspace was measured using the CPC. Median dry particle weight in the exposure airspace was measured using the DataRAM-4, and verified by the gravimetric filter readings taken during each exposure run. Estimated lung burden in the alveolar region was calculated using the following equation:

$$\begin{aligned}\text{Lung burden} &= (\text{MV}) \times (\text{T}) \times (\text{CON}) \times (\text{DF}) \\ &= (190\ \text{ml/min})(300\ \text{min}) \\ &\quad (100 \text{ or } 1000\ \mu\text{g/m}^3) \\ &\quad (1\ \text{m}^3/1,000,000\text{ml})\ (0.25)\end{aligned}$$

where (MV) is the minute ventilation of the exposed animal (ml/min); (T) is the total exposure time (min); (CON) is the average exposure concentration in ($\mu g/m^3$); and (DF) is the pulmonary deposition fraction for the alveolar region for the particles inhaled. A minute ventilation of 190 ml/min was used because this value is typical for the average age, weight, and strain of lab rat used in this study; however, it should be noted that this variable is dependent on a number of factors that may vary among the rats from a given lot, including, but not limited to, weight and activity level in the cage during exposure. The value for the DF was extrapolated from validated lung deposition curves for the rat model (Raabe et al., 1976; Anjilvel and Asgharian, 1995; Freijer et al., 1999; Winter-Sorkina and Cassee, 2003), based on the MAD of the particles, the minute ventilation of a rat, and the fractional residual lung capacity of a rat. Although there is a degree of uncertainty in the published deposition curves, these data provide the basis for an estimation of the total acinar deposition. Therefore, lung burdens were estimated to be 0, 1.4 or 14 μg/rat for control, low-dose, and high-dose animals, respectively.

Recorded runs lasting 5 h of exposure to the high-dose, low-dose, and control solutions are displayed in Figure 3. All three exposure runs had temperatures in the range of 22.7 to 23.3°C, and relative humidity from 70 to 75%. The particles were not dried fully before entering the exposure chamber because it is believed that a "wet" particle mimics more closely the type of nano Ag particle produced during consumer aerosol spray-on use.

TABLE 1. Study Exposure Conditions

Exposure type	Count median aerodynamic diameter	Weight of Ag in solution	Exposure chamber dry mass concentration	Exposure chamber wet particle concentration (number/ml)	Estimated lung burden
High dose	39 nm	200 mg/L	1000 $\mu g/m^3$	2100×10^3	14 μg
Low dose	33 nm	20 mg/L	100 $\mu g/m^3$	550×10^3	1.4 μg
Controls	27 nm	0 mg/L	<5 $\mu g/m^3$	350×10^3	0 μg

Note. All exposures were 5 h for 1 d. Lung burdens are estimations derived from use of an average minute ventilation for a given age, weight, and rat strain and a DF for a given particle size.

Aerosol Sizing

Particle distribution and morphology of the aerosols inside the exposure chamber were determined with a scanning mobility particle sizer (TSI, SMPS model 3034) and scanning electron microscopy (JEOL 6400, JEOL, Inc., Tokyo, Japan). The particle size distributions for each of the three exposure types are represented in Figure 4 with particle diameter (μm) on the *x* axis and a normalized number of particles on the *y* axis. The median particle count size was approximately 33 and 39 nm, according to the instrument, for low and high doses, respectively. The control dose for both particle concentrations had a slightly smaller size distribution of water droplets with a median particle size of 27 nm. The images in Figure 5 show the morphology of dry Ag particles collected from the exposure chamber using the low dose solution (MesoSilver) onto a polycarbonate filter; the images in Figure 6 show the dry Ag particles collected from the exposure chamber using the high-dose solution (NIST). The most common physical diameter of the Ag particles on both filters was in the 30 to 80 nm range.

Animals

Male Sprague-Dawley (Hla: SD CVF) rats weighing approximately 300 g (9 wk of age), obtained from Hilltop Labs (Scottdale, PA), were used in accordance with a protocol approved by the Institutional Animal Care and Use Committee. Animals were given a Teklad 2918 diet and tap water ad libitum, housed in a clean-air and viral- and antigen-free room with restricted access in an Association for Assessment and Accreditation of Laboratory Animal Care International (AAALAC)-approved animal facility under a 12 h:12 h light: dark cycle, and allowed to acclimate for 1 wk prior to use. Two sets of exposures with paired controls were conducted for each dose. For each exposure set and each dose, 12 rats were exposed to air ($n = 6$ for d 1 and $n = 6$ for d 7) and 12 rats were exposed to Ag particles ($n = 6$ for d 1 and $n = 6$ for d 7). Rats from one set of exposures were euthanized at d 1 and 7 for pulmonary response and microvascular studies. Rats from the second set of exposures were euthanized at d 1 and 7 following measurements for hemodynamic response study. Rats were randomized as they were added to the exposure chambers and at selection for rats designated for d-1 studies.

Measurement of Pulmonary Responses

On d 1 and 7, in rats from the first set of exposures to Ag nanoparticles or air, bronchoalveolar lavage (BAL) was performed by washing the lungs with aliquots of phosphate-buffered saline (PBS) in order to obtain pulmonary cells for morphological and functional analysis, and the acellular lavage fluid was retained for analysis of indicators of tissue damage and cellular activity, as described previously by Roberts et al. (2011) ($n = 6$ per group per time point per dose). Rats were euthanized with an overdose of sodium pentobarbital (>100 mg/kg; Sleepaway; Fort Dodge Animal Health, Madison, NJ), trachea was cannulated, chest cavity was opened, left lung was clamped off, and BAL was performed via the tracheal cannula. The acellular fraction of the first lavage was obtained by filling the lung with 2 ml/100 g body weight PBS, massaging

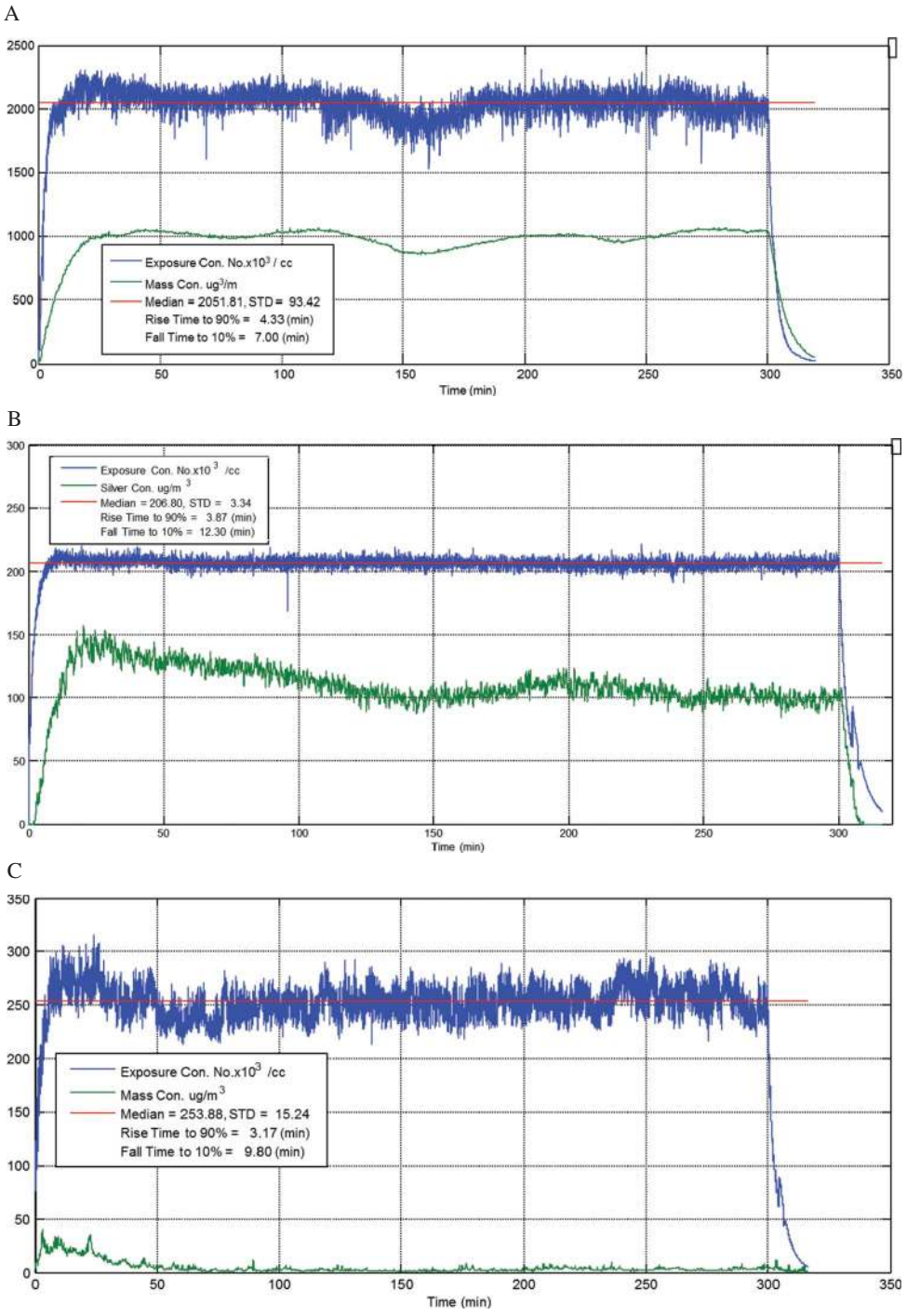

FIGURE 3. Exposure chamber concentration data for the high dose (NIST sample; 200 mg/L) aerosol exposure (A), the low-dose (MesoSilver sample; 20 mg/L) aerosol exposure (B), and the control (deionized water) aerosol exposure (C). Particle number ($\times 10^3$) and particle mass ($\mu g/m^3$) are given on the *y* axis (color figure available online).

for 30 s, withdrawing, and repeating the process one more time. This concentrated aliquot was withdrawn, retained and kept separately, and designated as the first fraction of BAL fluid (BALF). The subsequent aliquots were 6 ml in volume, instilled once with light massaging,

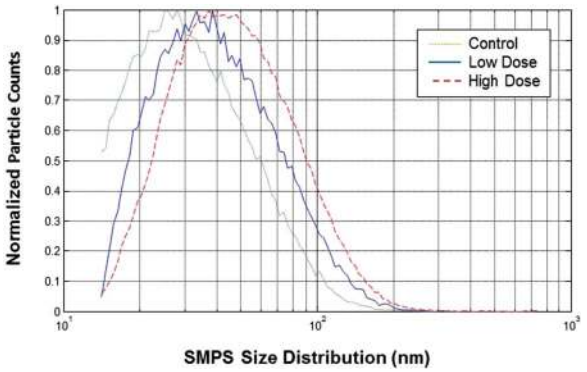

FIGURE 4. Aerosol particle size distribution data from the SMPS (scanning mobility particle sizer) collected from inside the exposure chamber (color figure available online).

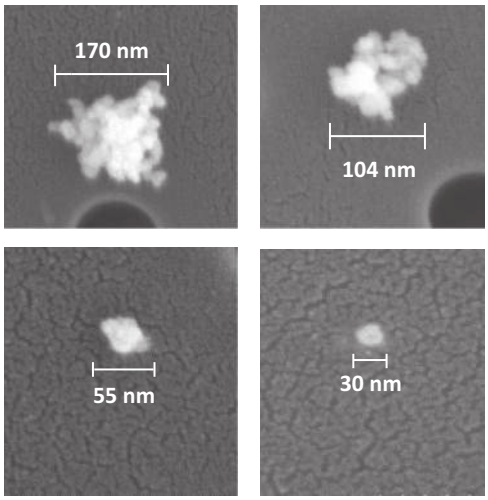

FIGURE 5. Scanning electron microscopy images of dry nano silver particles collected from inside the exposure chamber on a polycarbonate filter during the low dose exposure. The most commonly observed particle sizes were 30–80 nm.

withdrawn, and combined until a 30-ml volume was obtained. For each animal, both lavage fractions were centrifuged (10 min, 1200 × g); the cell pellets were combined and resuspended in 1 ml PBS; and the acellular fluid from the first lavage fraction was retained for further analysis.

The presence of albumin and the lactate dehydrogenase (LDH) activity in BALF of rats after exposure to air or Ag were measured to evaluate the loss of integrity of the alveolar–capillary barrier and general cytotoxicity, respectively. Measurements of both albumin and LDH activity in the acellular fluid were

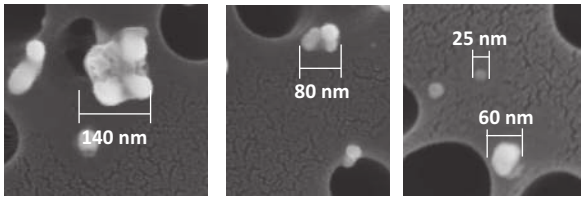

FIGURE 6. Scanning electron microscopy images of dry nano silver particles collected from inside the exposure chamber on a polycarbonate filter during the high dose exposure. The most commonly observed particle sizes were 30–80 nm.

obtained using a Cobas C111 clinical chemistry analyzer (Roche Diagnostic Systems, Montclair, NJ). Albumin was determined by spectrophotometric measurement of the reaction product of albumin with bromcresol green according to a method indicated by Sigma Diagnostics (St. Louis, MO). LDH activity was quantified by detection of the oxidation of lactate, coupled to the reduction of NAD+ at 340 nm.

The total number of BAL cells and the total number of alveolar macrophages (AM) collected from rats exposed to air or Ag were counted using size fractionation on a Coulter Multisizer II (Coulter Electronics; Hialeah, FL) for use in cell differential counts and for use in the chemiluminesence (CL) assay. Cell differentials were performed to determine the total number of AM, neutrophils, lymphocytes, and eosinophils. Briefly, 10^5 cells from each rat were spun down onto slides with a Cytospin 3 centrifuge (Shandon Life Sciences International; Chesire, England) and labeled with Leukostat stain (Fisher Scientific, Pittsburgh, PA) to differentiate cell types. Two hundred cells per slide were counted, and percentages of AM, neutrophils, lymphocytes, and eosinophils were multiplied by the total number of cells to calculate the number of each cell type.

To estimate phagocyte oxidant production, luminol-dependent CL was performed on BAL cells as a measure of light generated by the production of reactive oxygen species (ROS) by AM and neutrophils using a Berthold LB953 luminometer (Wallace Inc., Gaithersburg, MD) as described previously by Antonini et al. (1994). Baseline oxidant production by the cells was measured in the absence

of a stimulant. Phorbol 12-myristate 13-acetate (PMA) (10 μmol/L), a soluble stimulant of total BAL phagocytes (AM and neutrophils), or nonopsonized, insoluble zymosan (2 mg/mL), a stimulant of only AM (Castranova et al. 1990), was added to the assay immediately prior to CL measurement to determine the contribution of both AM and neutrophils to the overall production of ROS in the lungs of the rats. Measurement of CL was recorded for 15 min at 37°C, and the integral of counts per minute (cpm) per 10^6 cells versus time was calculated. CL was calculated as cpm of stimulated cells minus cpm of corresponding resting cells. The values were normalized using the Coulter counter measurements for total number of BAL cells (reflecting AM plus neutrophils) for PMA-stimulated CL and to number of AM in the BAL for zymosan-stimulated CL.

Blood Studies

Blood samples were obtained from anesthetized rats prior to BAL to evaluate the potential for a systemic inflammatory response to inhalation of nano Ag indicated by increased white blood cell populations. On d 1 and 7 postexposure, white blood cells (neutrophils, lymphocytes, monocytes, and eosinophils) were counted and differentiated using a Hemavet 950 veterinary multispecies hematology system (Drew Scientific Group, Dallas, TX).

In Vitro Microvessel Measurements

As described previously by Krajnak et al. (2011), tails were dissected from rats used in the pulmonary response studies ($n = 6$ rats per group per dose per time point) after exsanguination and placed in cold Dulbecco's modified Eagle's medium with glucose (Invitrogen/Gibco; Carlsbad, CA). Ventral tail arteries from the C14–C15 region of the tail were dissected shortly after euthanasia, mounted on glass pipettes in a microvessel chamber (Living Systems; Burlington, VT), and perfused with biocarbonated-HEPES buffer warmed to 37°C. Arteries were pressurized to 60 mm Hg and allowed to equilibrate for approximately 1 h. Phenylephrine (PHEN, α-1 adrenoreceptor agonist)-mediated vasoconstriction and acetylcholine (ACh)-mediated redilation were assessed. Krajnak et al. (2006, 2010, 2011) previously used these methods and doses of PHEN and ACh to demonstrate changes in vascular responsiveness as indicators of endothelial cell dysfunction. PHEN was applied to the chamber in half-log increments (−8.5 to −6.5 log mol/L) and the internal diameter was recorded after vessels stabilized (approximately 5 min between application of doses). Because ventral tail arteries usually display little basal tone, endothelial-mediated redilation was assessed after constriction with PHEN by adding ACh in half-log increments (−8.0 to −5.5 mol/L) using the procedures that were used to apply PHEN.

In Vivo Hemodynamic Measurements

Rats in exposure sets designated for hemodynamic studies ($n = 6$ rat per group per time point per dose) were anesthetized prior to catheterization with inhaled 2% isoflurane mixed with oxygen at a flow rate of 2 L/min as described previously (Krajnak et al., 2011). Using aseptic technique, a custom catheter, made according to the method described by Wang et al. (2004), was inserted into the left ventricle through the carotid artery. The correct position of the catheter tip in the left ventricle was confirmed by the waveform of the left ventricular pressure visualized on a computer monitor. Heart function was assessed by measuring maximal left ventricular systolic pressure (LVSP). To study vascular function, in vivo systemic arterial blood pressure (BP) was determined by using a fluid-filled arterial catheter that was placed in the femoral artery and connected to a pressure transducer coupled to a computerized cardiovascular continuous monitoring system (a PowerLab/4SP analog-to-digital converter; AD Instruments, Chalgrove, UK). Another catheter (polyurethane, 2 French size) was inserted into the jugular vein for the administration of isoproterenol (ISO) or norepinephrine (NE). Both chemicals were purchased from Sigma-Aldrich (St. Louis, MO). All three catheters were

exteriorized through subcutaneous tunneling and suturing on the back. The arterial catheters were connected to a fluid-filled pressure transducer for at least 20 min prior to measurements being made (or until rats displayed stable heart rate and BP measures). Heart rate (HR) and BP were recorded and analyzed using cardiovascular continuous monitoring software (PowerLab/4SP, AD Instruments, Colorado Springs, CO). Cardiopulmonary responses and spinal reflexes were monitored to determine that the proper depth of anesthesia was maintained. Each rat was euthanized with carbon dioxide after measurements were completed.

Statistical Analysis

Results are expressed as mean ± standard error of the mean (SEM) or standard deviation (STD), depending on the analysis. Aerosol concentration in the exposure chambers was collected over time during actual exposures, and mean concentration ± standard deviation during the exposure was calculated by a custom script generated in MATLAB (The MathWorks, Inc.).

Statistical analyses for blood cells and lung toxicity data were carried out with a SigmaStat 11.0 statistical program (Chicago, IL). The significant differences between Ag-exposed rats at a given dose and their paired controls were evaluated at each time point using analysis of variance (ANOVA). Significance was set at $p < .05$. The analyses of measures of BP, HR, and LSVP in response to dose-dependent changes in ISO and NE were generated using SAS/STAT software, version 9.1, of the SAS system for Windows (SAS Institute, Inc., Cary, NC). Dose-dependent changes in the internal diameter of ventral-tail arteries in response to stimulation with PHEN or Ach were analyzed using Jmp 5.1 (SAS Institute, Inc., Cary, NC). PROC MIXED (SAS Institute, Inc., Cary, NC) was utilized to run a two-way factorial analysis of variance with the concentration of ISO or NE as a repeated measure to account for multiple measures in individual animals. Treatment comparisons were then calculated at each level of drug utilizing the "slice" option. Dose responses to PHEN and ACh were analyzed using repeated measures of variance where the concentration of PHEN or ACh was used at the repeated measure. Measures collected from rats 1 and 7 d after exposures were performed separately. Treatment comparisons were made with Student's *t*-test. All statistical tests were considered significant at $p < .05$.

RESULTS

Pulmonary Response

LDH activity and albumin concentration were measured in the acellular first fraction of BAL fluid recovered from rats 1 d and 7 d post exposure to a low- or a high-dose Ag spray aerosol as indices of lung cell cytotoxicity and alveolar permeability, respectively (Figure 7). There were no significant differences in LDH activity (Figure 7A) or albumin levels (Figure 7B) in the low or high dose of silver spray aerosol groups when compared to respective air controls. Lung cells recovered by BAL were differentiated and counted to evaluate the inflammatory potential of Ag spray exposure (Table 2). The numerical increase in the number of neutrophils present in the BAL samples recovered from rats exposed to the high dose of Ag spray aerosol on d 1 and 7 post exposure when compared to respective air control group was not significantly different. There were no significant differences in total number of cells recovered by BAL or in numbers of macrophages or lymphocytes when comparing Ag spray groups to their controls. No eosinophils were detected in any of the treatment groups. Chemiluminescence was performed on BAL cells recovered by lavage 1 and 7 d postexposure to assess oxidant potential in the lung. There were no significant differences in either PMA-stimulated or zymosan-stimulated oxidant production by BAL cells among groups (data not shown).

Hematology

Leukocyte differentials were evaluated in blood collected at d 1 and 7 post exposure to

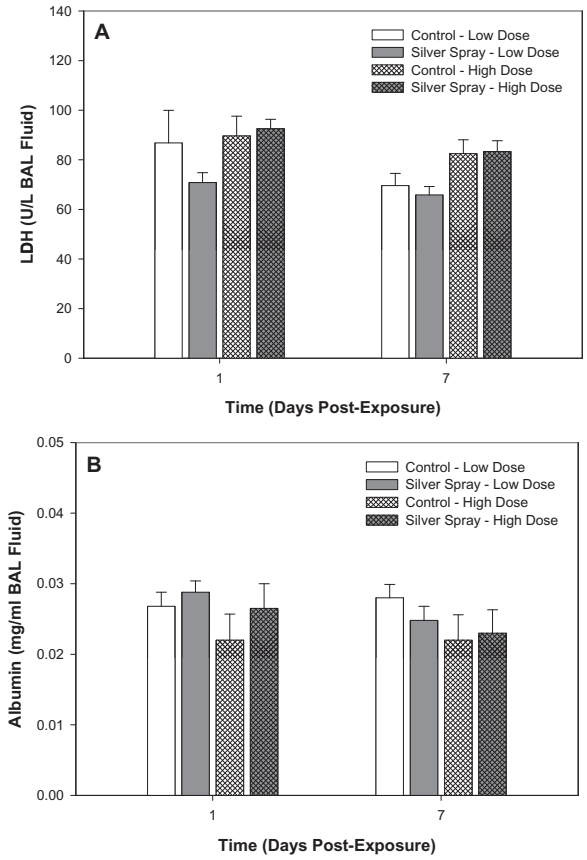

FIGURE 7. Lactate dehydrogenase (LDH) activity (A) and albumin concentration (B) in the acellular first fraction of BAL fluid collected from rats 1 and 7 d after exposure to a low or a high dose of silver spray aerosol, or filtered air as a control ($n = 6$ per group per time point) as a measure of cytotoxicity and lung injury. There were no significant differences in animals exposed to the high or low doses of silver spray aerosol when compared to their respective control group. Values are means ± SEM ($n = 6$ per group per time point).

the low- and high-dose Ag spray aerosols relative to respective air control (Table 3). There was a significant increase in blood monocytes on d 1 after exposure to the high dose of Ag spray. There was also a quantitative rise in blood monocytes on d 1 after exposure to the low dose of Ag spray, although this did not differ statistically from the control. There were no significant differences at either time point in regard to lymphocyte, neutrophil, or eosinophil number in the blood collected from animals exposed to the high or low dose of Ag spray aerosol.

In Vitro Microvessel Measurements

The dose-dependent vasoconstriction induced by PHEN was similar in arteries from control and exposed rats at both doses (data not shown). Exposure to the low dose of Ag spray resulted in a significant reduction in vascular responsiveness to ACh-induced redilation on d 1 after the exposure (Figure 8A). However, this difference was no longer apparent 7 d after the low-dose exposure (Figure 8B). Although arteries from rats exposed to the high dose of Ag spray also appeared to display numerically reduced sensitivity to ACh-induced redilation 1 d after inhalation exposure, this difference was not significant. There also was no treatment difference in ACh-induced redilation in arteries collected from rats 7 d after high dose exposure (Figure 8C).

In Vivo Cardiovascular Responses

Pulmonary inhalation of Ag spray did not markedly change basal HR, maximum LVSP, or mean BP (MBP) compared to control (exposed to filtered air) at 1 or 7 d postexposure (data

TABLE 2. Bronchoalveolar (BAL) Cell Differentials

Time Post-Exposure	Exposure Group	Total BAL Cells (10^5)	Macrophages (10^5)	Neutrophils (10^5)	Lymphocytes (10^5)
Day 1	Control - Low Dose	110 ± 7.30	109 ± 7.12	0.03 ± 0.02	0.22 ± 0.22
	Silver Spray - Low Dose	113 ± 7.12	112 ± 7.11	0.09 ± 0.09	0.55 ± 0.21
	Control - High Dose	121 ± 7.12	121 ± 7.14	0.29 ± 0.13	0.00 ± 0.00
	Silver Spray - High Dose	106 ± 9.79	105 ± 9.79	0.50 ± 0.20	0.08 ± 0.08
Day 7	Control - Low Dose	113 ± 3.50	112 ± 3.41	0.18 ± 0.12	0.46 ± 0.17
	Silver Spray - Low Dose	120 ± 7.57	119 ± 7.59	0.20 ± 0.13	0.57 ± 0.15
	Control - High Dose	124 ± 7.84	123 ± 7.91	0.38 ± 0.13	0.09 ± 0.09
	Silver Spray - High Dose	119 ± 6.07	118 ± 6.06	0.67 ± 0.18	0.00 ± 0.00

Note. Values are means ± SEM ($n = 6$ per group per time point.).

TABLE 3. Leukocyte Differentials in Blood

Time Post-Exposure	Exposure Group	Total WBC (K/uL)	Monocytes (K/uL)	Lymphocytes (K/ul)	Neutrophils (K/uL)	Eosinophils (K/uL)
Day 1	Control - Low Dose	6.296 ± 0.730	0.246 ± 0.045	4.686 ± 0.655	1.358 ± 0.158	0.006 ± 0.002
	Silver Spray - Low Dose	6.870 ± 0.775	0.360 ± 0.040	4.472 ± 0.589	1.712 ± 0.179	0.014 ± 0.007
	Control - High Dose	5.333 ± 0.346	0.165 ± 0.027	3.950 ± 0.263	1.210 ± 0.119	0.008 ± 0.002
	Silver Spray - High Dose	5.567 ± 0.397	0.280 ± 0.024*	3.570 ± 0.181	1.707 ± 0.333	0.010 ± 0.003
Day 7	Control - Low Dose	6.20 ± 0.27	0.288 ± 0.040	4.702 ± 0.205	1.200 ± 0.106	0.005 ± 0.002
	Silver Spray - Low Dose	5.92 ± 0.50	0.255 ± 0.032	4.515 ± 0.374	1.142 ± 0.136	0.010 ± 0.006
	Control - High Dose	6.873 ± 0.652	0.332 ± 0.055	4.805 ± 0.510	1.723 ± 0.223	0.010 ± 0.004
	Silver Spray - High Dose	6.070 ± 0.547	0.345 ± 0.026	4.343 ± 0.400	1.372 ± 0.173	0.003 ± 0.002

Note. Values are means ± SEM ($n = 6$ per group per time point.); asterisk indicates significantly different from corresponding control group ($p < .05$).

not shown). HR in response to the highest dose of ISO was increased significantly only at 1 d postexposure to the low concentration of Ag spray (Figure 9A). LVSP in response to ISO was reduced only at 7 d postexposure at the high dose of Ag spray (Figure 9B). Alteration in response to β-adrenergic stimulation is a common characteristic of cardiac dysfunction; however, the alterations in HR and LVSP only occurred in response to the highest does of ISO, suggesting that pulmonary inhalation of Ag spray exerted only a minor effect on the heart. The impact of inhalation of Ag nanoparticles on vascular function was assessed by monitoring MBP. There was no marked effect of Ag spray inhalation on MBP in response to NE (Figure 9C). These results indicate that compensatory mechanisms of the cardiovascular system were sufficient to overcome minor changes in vascular function induced by inhalation of Ag spray.

DISCUSSION

In this study, rats were exposed by inhalation to a wet aerosol of Ag nanoparticles at a lung burden of either 1.4 μg/rat or 14 μg/rat. No significant cytotoxicity (BAL LDH activity) or air/blood-barrier damage (BAL albumin level) was noted at 1 or 7 d post exposure to either dose. Similarly, BAL differential cell counts and BAL cell activity (chemiluminescence) were unaffected by Ag nanoparticles. The increase in BAL neutrophils (1.75-fold above control at 1 and 7 d postexposure) was not found to be statistically significant. With the exception of a significant 1.7-fold rise in blood monocytes 1 d after exposure to the high dose of Ag, differential blood counts were not markedly changed following pulmonary exposure to Ag nanoparticles. Inhalation of Ag nanoparticles did not markedly affect vasoconstriction of the tail artery in response to PHEN, or basal HR, maximal LVSP, or MBP. However, a decreased dilation of tail artery in response to ACh and an increase in heart rate in response to ISO were noted 1 d after low-dose Ag exposure. Such changes were not seen after high-dose exposure on d 1 or 7 post exposure to either the high or low dose. The presence of slight cardiovascular changes seen at Ag burdens of 1.4 μg/rat but not 14 μg/rat may be due to the fact that a substantial fraction of the commercial spray used for low-dose exposure was ionic rather than particulate Ag, in contrast to the NIST sample used for the high-dose exposure. Therefore, it is possible that ionic Ag translocated to cardiovascular tissue, producing these low-level responses. Nevertheless, at lung burdens achieved in the present study, in general no striking pulmonary or cardiovascular changes were observed.

Recently, a wet aerosol study related to TiO_2 spray exposure was conducted by our lab. In that study, inhalation of a wet aerosol nano TiO_2 from a commercial antimicrobial spray product increased neutrophils harvested by BAL of rats by 2.1-fold above control levels at 1 d postexposure (McKinney et al., 2012). This

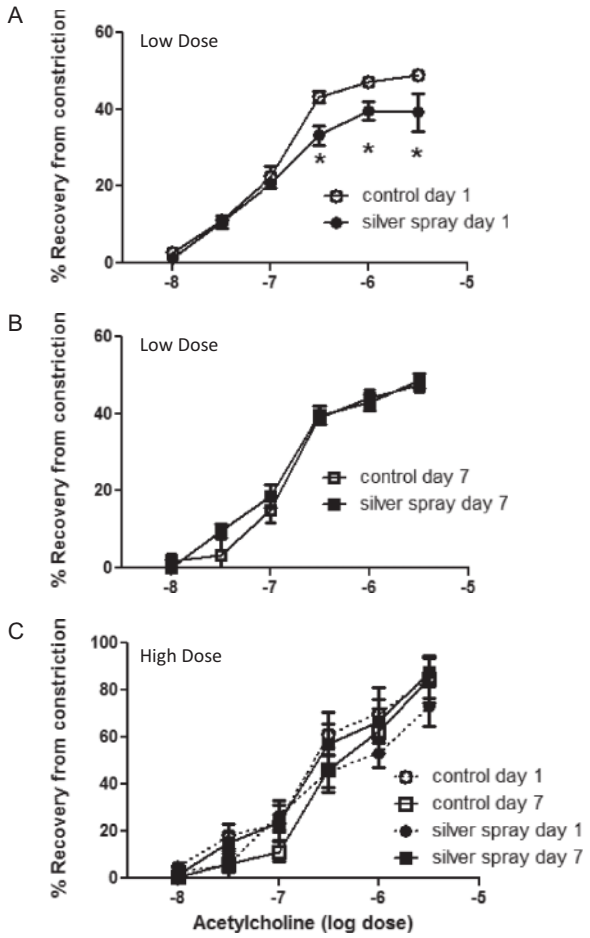

FIGURE 8. Acetylcholine (Ach)-induced redilation of ventral tail arteries after inhalation of low- and high-dose silver spray. Exposure to the low-dose silver spray (A) resulted in a reduction in sensitivity of arteries to ACh-induced redilation 1 d after the exposure (asterisk indicates different from controls, $p < .05$), but this effect was no longer apparent 7 d after the exposure (B). Inhalation of the high dose of silver spray did not result in any significant differences in ACh-induced redilation at 1 or 7 d after the exposure (C). Values are means ± SEM ($n = 6$ per group per time point).

animal model was identical to that employed for the current Ag spray study with regard to animal age/weight, duration of exposure, and times postexposure; however, the target TiO_2 concentration was higher. Nano TiO_2 lung burdens achieved were 43 μg/rat. In the present study, despite a lack of statistical significance, inhalation of the high dose of nano Ag (lung burden 14 μg/rat) increased BAL neutrophils by 1.75-fold above control at 1 d postexposure, a rise that may be amplified at an equivalent lung burden as that attained for TiO_2. Based on the current TLV-TWA for TiO_2 (10 mg/m^3) versus particulate Ag (0.1 mg/m^3), the potentially greater potency of Ag versus TiO_2 in wet aerosol form is not surprising. The potential difference in potency may be due to the presence or liberation of ions from the Ag particles as compared to a relatively insoluble TiO_2, which may subsequently lead to an elevation in oxidant production at levels sufficiently high to damage cell membranes. It is well understood that soluble Ag is considered to be more toxic than coarse or fine particulate, as reflected in the respiratory regulation by the ACGIH for soluble Ag (0.01 mg/m^3) versus the particulate form (0.1 mg/m^3).

Indeed, cell damage from nano Ag was associated with ROS generated by ionic Ag (Kittler et al., 2010), while nano TiO_2, in the absence of UV irradiation, failed to generate substantial ROS both in the absence and in the presence of macrophages (Rushton et al., 2010). In addition, there have been several studies that showed that the mode of action of Ag nanoparticles against pathogens is related to their size, shape, and surface area, allowing for a greater surface for release of Ag ions and generation of free radicals (Wijnhoven et al., 2009). There are numerous factors affecting solubility of Ag nanoparticles, including, but not limited to, size (Ma et al., 2012), surface coating (Li et al., 2012; Tejamaya et al., 2012; Zook et al., 2011), pH (Elzey and Grassain 2010; Rogers et al., 2012), and the solution concentration of sulfur (Levard et al., 2011) or sodium chloride (Kent and Vikesland, 2012). The multitude of factors renders an estimation of the dissolution of the commercial product used in this study difficult, as the amount of ion versus particle may change measurably in the time between manufacturing and end use. However, the preparation of the sample from NIST was known to be almost entirely particulate at the time of exposure, and this sample as a wet aerosol did not produce significant alterations in pulmonary or cardiovascular responses.

Several inhalation studies examined respiratory exposure to aerosols generated from Ag in the dry powder form, where only

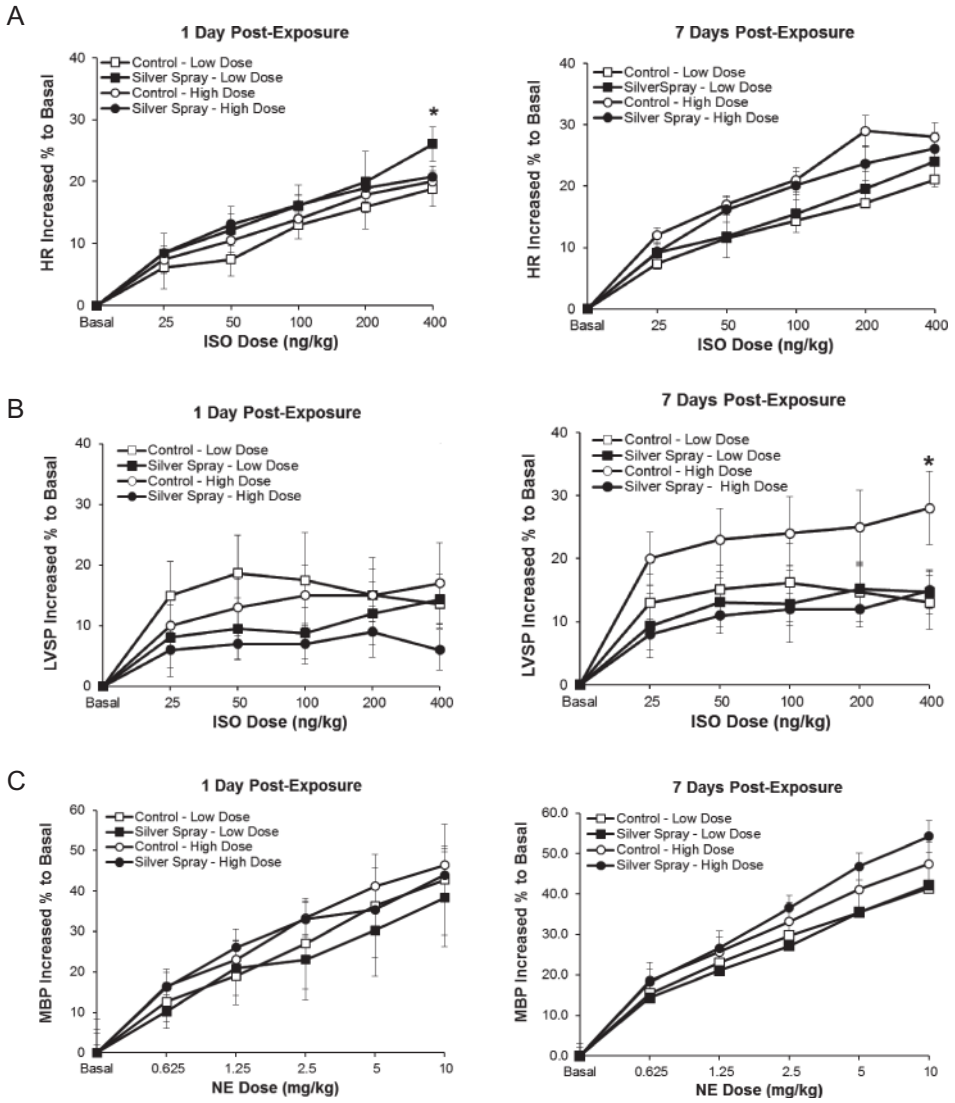

FIGURE 9. Cardiovascular changes after pulmonary exposure to silver spray. (A) Heart rate (HR) changes in response to isoproterenol (ISO). (B) Left ventricular systolic pressure (LVSP) in response to ISO. (C) Mean blood pressure (MBP) in response to norepinephrine (NE). Values are means ± SEM ($n = 6$ per group per time point.). Asterisk indicates a significant difference between silver spray and the air control group ($p < .05$).

the highest doses (5- to 7-fold higher than the TLV-TWA of 0.1 $\mu g/m^3$) for durations greater than 1 mo produced adverse pulmonary effects. In an inhalation dose-response study, Sung et al. (2009) reported that exposure of rats to the highest dose of aerosolized Ag nanoparticles used (515 $\mu g/m^3$, 6 h/d, 5 d/wk for 13 wk or 65 d) produced histopathological changes that included the following: alveolar inflammation, small granulomatous lesions in the lung, and bile-duct hyperplasia in the liver. When exposure duration was increased to 90 consecutive days, decreases in tidal volume and minute ventilation were noted, in addition to the alveolar inflammation and small granulomas reported after the 13-wk (5 d/wk or 65 d) inhalation (Sung et al., 2008). Decreases in lung function and pulmonary inflammation recovered to normal levels 12 wk after cessation of inhalation exposure in female rats, while recovery was incomplete in male rats (Sung et al., 2013). It should be noted that total lung

burdens in the Sung et al. (2009) study were as much as 40-fold greater than those achieved in the present investigation due to a longer duration of exposure and higher doses. In the Sung et al. (2009) study, a no-observable-effect limit (NOEL) of 100 $\mu g/m^3$ for 13 wk (5 d/wk) of inhalation exposure was reported. Whether the lung toxicity observed at the high doses in the studies discussed earlier was due to ion release over time in lung or the particle itself is difficult to determine.

Inhalation studies employing lower aerosol levels and/or shorter durations of exposure reported no marked changes in blood cell differentials or blood chemistry, and minimal lung inflammation (Ji et al., 2007; Stebounova et al., 2011). A dry powder aerosol study with comparable Ag particle size, dose, and exposure duration to the present one was performed by Sung et al. (2011). In this study, rats were exposed for 4 h to one of 3 doses of dry powder Ag aerosol (18–20 nm diameter Ag particles): 76, 135, or 750 $\mu g/m^3$. Lung function, body weight, and organ weights were monitored at various time points for up to 2 wk following exposure. No marked effects were observed. Similarly, no statistically significant pulmonary changes were reported in the current inhalation study examining wet aerosols of Ag, and only minor cardiovascular changes were observed with the low-dose commercial spray product which likely contained Ag ion. No alterations in cardiovascular measures were found with the high-dose Ag spray which was known to contain little soluble Ag relative to particle content. These studies taken together indicate that acute inhalation exposure to particulate Ag in the size range of approximately 20–60 nm at doses of up 1000 $\mu g/m^3$ poses minimal cardiopulmonary hazard, whether the aerosol is a dry powder or a wet spray. However, this may not be the case if the wet aerosol contains significant amounts Ag ions, as may be the case in the commercial product used in this study, and the concentration of the ion fraction is high enough to induce toxicity. Further investigation of exposure to wet aerosols from spray products with different particle:ion ratios and concentrations is warranted.

REFERENCES

Anjilvel, S., and Asgharian, B. 1995. A multiple-path model of particle deposition in the rat lung. *Fundam. Appl. Toxicol*. 28: 41–50.

Antonini, J. M., Van Dyke, K., Ye, Z., DiMatteo, M., and Reasor, M. J. 1994. Introduction of luminol-dependent chemiluminescence as a method to study silica inflammation in the tissue and phagocytic cells of rat lung. *Environ. Health Perspect*. 102(suppl. 10): 37–42.

Beckerman, B. S., Jerrett, M., Finkelstein, M., Kanaroglu, P., Brook, J. R., Arain, M. A., Sears, M. R., Stieb, D., Balmes, J., and Chapman, K. 2012. The association between chronic exposure to traffic-related air pollution and ischemic heart disease. *J. Toxicol. Environ. Health A* 75: 402–411.

Castranova, V., Jones, T., Barger, M., Afshari, A., and Frazer, D. G. 1990. Pulmonary responses of guinea pigs to consecutive exposures to cotton dust. In *Proceedings of the 14th Cotton Dust Research Conference*, ed. R. R. Jacobs, P. J. Wakelyn, and L. N. Domelsmith, 131–135. Memphis, TN: National Cotton Council.

Chen, B. T., Afshari, A., Stone, S., Jackson, M., Schwegler-Berry, D., Frazer, D. G., Castranova, V., and Thomas, T. A. 2010. Nanoparticles-containing spray can aerosol: Characterization, exposure assessment, and generator design. *Inhal. Toxicol*. 22: 1072–1082.

Elzey, S., and Grassian, V. H. 2010. Agglomeration, isolation, and dissolution of commercially manufactured silver nanoparticles in aqueous environments. *J. Nanoparticle Res*. 12: 1945–1958.

Freijer, J. I., Cassee, F. R., Subramaniam, R., Asghararian, B., Anjilvel, S., Miller, F. J., van Bree, L., and Rombout, P. J. A. 1999. Multiple Path Particle Deposition Model (MPPDep Version 1.11). A model for human and rat airway particle deposition. RIVM Report 650010019. http://www.rivm.nl/bibliotheek/rapporten/650010019.html

Hsieh, Y.-L., Yang, Y.-H., Wu, T.-N. and Yang, C.-Y. 2010. Air pollution and hospital

admissions for myocardial infarction in a subtropical city: Taipei, Taiwan. *J. Toxicol. Environ. Health A* 73: 757–765.

Ji, J. H., Jung, J. H., Kim, S. S., Yoon, J. U., Park, J. D., Choi, B. S., Chung, Y. H., Kwon, I. H., Jeong, J., Han, B. S., Shin, J. H., Sung, J. H., Song, K. S., and Yu, I. J. 2007. Twenty-eight-day inhalation toxicity study of silver nanoparticles in Sprague-Dawley rats. *Inhal, Toxicol*. 19: 857–871.

Kent, R. D., and Vikesland, P. J. 2012. Controlled evaluation of silver nanoparticle dissolution using atomic force spectroscopy. *Environ. Sci. Technol*. 46:6977–6984.

Kittler, S., Greulich, C., Diendorf, J., Koller, M., and Epple, M. 2010. Toxicity of silver nanoparticles increases during storage because of slow dissolution under release of silver ions. *Chem. Mater*. 22: 4548–4554.

Krajnak, K., Dong, R. G., Flavahan, S., Welcome, D., and Flavahan, N. A. 2006. Acute vibration increases alpha2C-adrenergic smooth muscle constriction and alters thermosensitivity of cutaneous arteries. *J. Appl. Phys*. 100: 1230–1237.

Krajnak K., Waugh S., Johnson, C., Miller, R., and Kiedrowski, M. 2009. Vibration disrupts vascular function in a model of metabolic syndrome. *Ind. Health*, *47*: 533–542.

Krajnak, K., Kan, H., Waugh, S., Miller, G. R., Johnson, C., Roberts, J. R., Goldsmith, W. T., Jackson, M., McKinney, W., Frazer, D., Kashon, M. L., and Castranova, V. 2011. Acute effects of COREXIT EC9500A on cardiovascular function in rats. *J. Toxicol. Environ. Health* 74: 1397–1404.

Levard, C., Reinsch, B. C., Michel, F. M., Oumahi, C., Lowry, G. V., and Brown, G. E. 2011. Sulfidation processes of PVP-coated silver nanoparticles in aqueous solution: Impact on dissolution rate. *Environ. Sci. Technol*. 45: 5260–5266.

Li, X., Lenhart, J. J., and Walker, H. W. 2012. Aggregation kinetics and dissolution of coated silver nanoparticles. *Langmuir* 28: 1095–1104.

Liao, D., Shaffer, M. L., He, F., Rodriguez-Colon, S., Wu, R., Whitsel, E. A., Bixler, E. O., and Cascio, W. E. 2011. Fine particulate air pollution is associated with higher vulnerability to atrial fibrillation-the APACR study. *J. Toxicol. Environ. Health A* 74: 693–705.

Ma, R., Levard, C., Marinakos, S. M., Cheng, Y., Liu, J., Michel, F. M., Brown, G. E., and Lowry, G. V. 2012. Size-controlled dissolution of organic-coated silver nanoparticles. *Environ. Sci. Technol*. 46: 752–759.

MacCuspie, R. I., Allen, A. J., and Hackley, V. A. 2011. Dispersion stabilization of silver nanoparticles in synthetic lung fluid studied under *in situ* conditions. *Nanotoxicology* 5: 140–156.

Mann, E. E., Thompson, L. C., Shannahan, J. H., and Wingard, C. J. 2012. Changes in cardiopulmonary function induced by nanoparticles. *Rev. Nanomed. Nanobiotechnol*. 4:691–702.

McKinney, W., Jackson, M., Sager, T. M., Reynolds, J. S., Chen, B. T., Afshari, A., Krajnak, K., Waugh, S., Johnson, C., Mercer, R. R., Frazer, D. G., Thomas, T. A., and Castranova, V. 2012. Pulmonary and cardiovascular responses of rats to inhalation of commercial antimicrobial spray containing titanium dioxide nanoparticles. *Inhal. Toxicol*. 24: 447–457.

Nurkiewicz, T. R., Porter, D. W., Hubbs, A. F., Cumpston, J. L., Chen, B. T., Frazer, D. G., and Castranova, V. 2008. Nanoparticle inhalation augments particle-dependent systemic microvascular dysfunction. *Particle Fibre Toxicol*. 5: 1. doi:10.1186/1743-8977-5-1

Pope, C. A., Dockery, D. W., and Schwartz, J. 1995. Review of epidemiological evidence of health effects of particulate air pollution. *Inhal. Toxicol*. 7: 1–18.

Pope, C. A., Burnett, R. T., Thun, M.J., Calle, E. E., Krewski, D., Ito, K., and Thurston, G. D. 2002. Lung cancer, cardiopulmonary mortality, and long-term exposure to fine particulate air pollution. *J. Am. Med. Assoc*. 287: 1132–1141.

Qyadros, M. E., and Marr, L. C. 2011. Silver nanoparticles and total aerosols emitted by nanotechnology-related consumer spray products. *Environ. Sci. Technol*. 45:10713–10719.

Raabe, O. G., Yeh, H. C., Schum, G. M., and Phalen, R. F. 1976. Tracheobronchial geometry: Human, dog, rat, hamster (Report LF-53). Albuquerque, NM: Lovelace Foundation.

Roberts, J. R., Reynolds, J. S., Thompson, J. A., Zaccone, E. J., Shimko, M. J., Goldsmith, W. J., Jackson, M., McKinney, W., Frazer, D. G., Kenyon, A., Kashon, M. L., Piedimonte, G., Castranova, V., and Fedan, J. S. 2011. Pulmonary effects after acute inhalation of oil dispersant (COREXIT EC9500A) in rats. *J. Toxicol. Environ. Health A* 74: 1381–1396.

Rogers, K. R., Bradham, K., Tolaymat, T., Thomas, D. J., Hartmann, T., Ma, L., and Williams, A. 2012. Alterations in physical state of silver nanoparticles exposed to synthetic human stomach fluid. *Sci. Total Environ*. 420: 334–339.

Ruston, E. K., Jiang, J. Leonard, S. S., Eberly, S., Castranova, V., Biswas, P., Elder, A., Han, X., Gelein, R., Finkelstein, J., and Oberdorster, G. 2010. Concepts of assessing nanoparticle hazards considering nanoparticle dose and chemical/biological response metrics. *J. Toxicol Environ. Health* 73: 445–461.

Samet, J. M., Dominici, F., Curriero, F. C., Coursac, I., and Zeger, S. L. 2000. Fine particulate air pollution and mortality in 20 U. S. cities, 1987–1994. *N. Engl. J. Med*. 343: 1742–1749.

Simeonova, P. P., and Erdely, A. 2009. Engineered nanoparticle respiratory exposure and potential risks for cardiovascular toxicity: Predictive tests and biomarkers. *Inhal. Toxicol*. 21(suppl. 1):68–73.

Stebounova, L. V., Adamcakova-Dodd, A., Kim, J. S., Park, H., O'Shaghnessy, P. T., Grassian, V. H., and Thorne, P. S. 2011. Nanosilver induces minimal lung toxicity or inflammation in a subacute murine inhalation model. *Particle Fibre Toxicol*. 8: 5.

Sung, J. H., Ji, J. H., Yoon, J. U., Kim, D. S., Song, M. Y., Jeong, J., Han, B. S., Han, J. H., Chung, Y. H., Kim, J., Kim, T. S., Chang, H. K., Lee, E. L., Lee, J. H., and Yu, I. J. 2008. Lung function changes in Sprague-Dawley rats after prolonged inhalation exposure to silver nanoparticles. *Inhal. Toxicol*. 20:567–574.

Sung, J. H., Ji, J. H., Park, J. D., Yoon, J. U., Kim, D. S., Jeon, K. S., Song, M. Y., Jeong, J., Han, B. S., Han, J. H., Chung, Y. H., Chang, H. K., Lee, J. H., Cho, M. H., Kelman, B. J., and Ya, I. J. 2009. Subchronic inhalation toxicity of silver nanoparticles. *Toxicol. Sci*. 108: 425–461.

Sung, J.H., Ji, J.H., Song, S.K., Lee, J.H., Choi, K.H., Lee, S. H., and Yu, I. J. 2011. Acute inhalation toxicity of silver nanoparticles. *Toxicol. Ind. Health*. 27:149–154.

Sung, K. S., Sung, J. H., Ji, J. H., Lee, J. H., Lee, J. S., Ryu, H. R., Lee, J. K., Chung, Y. H., Park, H. M., Shin, B. S., Chang, H. K., Kelman, B., and Yu, I. L. 2013. Recovery from silver-nanoparticle-exposure-induced lung inflammation and lung function changes in Sprague-Dawley rats. *Nanotoxicology*. 7:169–180.

Tejamaya, M., Romer, I., Merrifield, R. C., and Lead, J. R. 2012. Stability of citrate, PVP, and PEG coated silver nanoparticles in ecotoxicology media. *Environ. Sci. Technol*. 46: 7011–7017.

Wang, Q., Brunner, H. R., and Burner, M. 2004. Determination of cardiac contractility in awake, unsedated mice with a fluid filled catheter. *Am. J. Physiol. Heart Circ. Physiol*. 286: H806–H814.

Wijnhoven, S. W. P., Peijenburg, W. J. G. M, Herberts, C. A., Hagens, W. I., Oomer, A. G., Heugens, E. H. W., Roszek, B., Bisschops, J., Gosens, I., Van Meent, D., Dekkers, S., De Jong, W. H., Van Zijnerden, M., Sips, A. J. A. M., and Geertsma, R. E. 2009. Nano-silver: A review of available data and knowledge gaps in human and environmental risk assessment. *Nanotoxicology* 3: 109–138.

Winter-Sorkina, R. D., and Cassee, F. R. 2003. From concentration to dose: factors influencing airborne particulate matter deposition in humans and rats. RIVM Report 650010031. http://rivm.openrepository.com/rivm/bitstream/10029/9272/1/650010031.pdf

Xue, C., Wu, J., Lan, F., Yang, X., Zeng, F., and Xu, H. 2010. Nano titanium dioxide induces the generation of ROS and potential damage in HaCaT cells under UVA irradiation. *J. Nanosci. Nanotechnol*. 10: 8500–8507.

Zook, J. M., Long, S. E., Cleveland, D., Geronimo, C. L., and MacCuspie, R. I. 2011. Measuring silver nanoparticle dissolution in complex biological and environmental matrices using UV-visible absorbance. *Anal. Bioanal. Chem*. 401: 1993–2002.